ARTICLES

Electric Impedance Spectroscopy of Titania: Influence of Gas Treatment and of Surface Area

Dominik Eder* and Reinhard Kramer

Institute of Physical Chemistry, University of Innsbruck, Innrain 52a, A-6020 Innsbruck, Austria

Received: September 15, 2003; In Final Form: June 25, 2004

The electric charge transport in oxygen-treated titania is accomplished via two different routes. One of these pathways (A) occurs by electronic transport through the bulk phase with additional contributions from transfer through grain boundaries and between the electrode and the grains. As a parallel conduction pathway (B) ions can move along the grain surface parallel to the electric field and can surmount the grain boundaries between the grains. Because of the low voltage applied, the ion discharge at the electrode by electrochemical reaction is impeded and contributes a capacitive impedance only. According to this mechanism an equivalent circuit model was proposed that fits excellently the experimental data. When samples with a low surface area are treated in oxygen, the charge is transported mostly by electrons via pathway A. The electrons are formed by removal of oxygen leaving a surface oxygen vacancy and two electrons in the titania. Since the formation of these charge carriers is highly endothermic, the apparent activation energy of this mechanism is higher than that of the ionic conduction and thus the ionic transport along the surface becomes more important at lower temperatures. The contribution of the ionic conduction becomes important only in samples with a high surface area. When titania is treated in hydrogen the conductance is drastically increased, since surface oxygen ions are removed more easily due to reaction with hydrogen. The apparent activation energy for electronic conduction becomes smaller because the enthalpy of vacancy formation is decreased by the formation energy of water. Thus, in hydrogen treated titania the conduction is accomplished exclusively by electronic transport.

1. Introduction

Titania exhibits several interesting properties when treated under reducing conditions. One of these effects is the increase in electric conductivity when the fugacity of oxygen is decreased.[1−8] This property is used in gas sensors for detecting oxygen as well as hydrogen in the surrounding gas.[9,10] But the reduction of titania also affects the catalytic performance of noble metal catalysts supported by titania, since treatment in hydrogen at temperatures above 673 K induces the so-called SMSI effect,[2,11−21] which is characterized by decreased adsorption capacity for hydrogen and carbon monoxide and a loss of activity for hydrocarbon skeletal reactions.[19]

It is accepted that these effects are due to the reducibility of titania. To study the extent of reduction we investigated the influence of time and temperature of the hydrogen treatment on the stoichiometry of the resulting titania.[22,23] It was found that during the hydrogen treatment surface oxygen vacancies and electrons are formed. The number of these vacancies is controlled by an equilibrium between the surface and the gas phase and can be adjusted by systematically varying the water vapor pressure in the flowing hydrogen gas.

In a recent paper[22] we investigated the overall conductance of titania as a function of hydrogen treatment conditions and obtained some evidence that the conductivity increase induced by this treatment relates to the number of electrons formed during reduction.

In this paper, we want to deconvolute the different resistive and capacitive contributions to the overall impedance by electric impedance spectroscopy. To explore the role of surface conduction we used two samples with a different surface area. One aim of this work was to clarify the mechanisms of conduction in titania, and the other, to obtain values of the electric properties of the bulk phase, the grain boundary, and the surface of titania.

2. Experimental Section

Materials. The titanium oxide used in this work was TiO_2-P25 supplied by Degussa, which consists predominantly of anatase. Before use, the titania was calcined in air at different temperatures, which was accompanied by sintering, leading to a systematically controlled surface area. The surface area of the samples was determined by adsorption of nitrogen at 77 K according to BET. Structural changes due to thermal and vacuum treatments were investigated by X-ray diffraction (XRD).

Two samples with different surface areas were studied. The titania defined as a "high-surface sample" with a BET surface area of 50 m^2/g consists of about 70% anatase and 30% rutile. X-ray line broadening analysis revealed a crystallite diameter of about 22 nm from anatase diffraction peaks and one of about 27 nm from rutile diffraction peaks, indicating a surface area of the crystallites of about 60 m^2/g. Consequently, more than

* E-mail: dominik.eder@uibk.ac.at.

10.1021/jp0367373 CCC: $27.50
Published on Web 08/26/2004

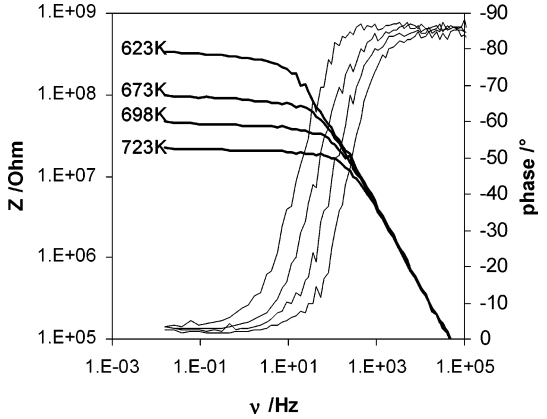

Figure 1. Bode diagram of the oxygen-treated low-surface sample as a function of temperature.

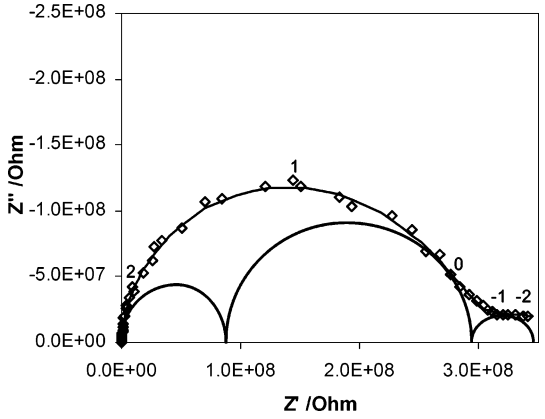

Figure 2. Nyquist-diagram of the low-surface sample treated in oxygen at 623 K (data points), and contributions of three serial RC elements and the resulting Nyquist spectrum calculated from these contributions (continuous line).

80% of the crystallite surface is accessible from the gas phase. This high-surface sample could only be treated up to temperatures of 773 K since sintering starts above these temperatures. In other experiments titania was calcined at 1073 K. This sintered titania exhibited a BET surface area of 1.5 m^2/g and is therefore denominated as a "low-surface sample". XRD analysis of the sintered sample showed that the structure was completely converted to rutile, the size of the crystallites being larger than 65 nm, as revealed by XRD line broadening. In this low-surface sample most of the pores were collapsed and less than 7% of the crystallite surface remained accessible to the gas phase.

Electrochemical Impedance Spectroscopy. The titania samples were pressed with about 3000 bar to produce pellets of about 1-mm thickness and 6-mm diameter. To enhance the electric contact, thin layers of gold were deposited on both sides of the pellets by high-vacuum deposition. The pellets were placed in a quartz glass tube equipped with gold electrodes that were pressed with 1 bar onto the pellet. The apparatus is suited for different gas treatments and is described elsewhere.[22] For some measurements a controlled water vapor pressure (6.1 mbar) was added by passing the gas flow through a trap in which water was held at 273 K. Heating to 1073 K was achieved by a tubular oven and controlled by a thermocouple (situated in the reactor about 5 mm downstream of the pellet).

The conductivity of the sample was measured by an IM5d impedance spectrometer (Zahner-Elektrik), supplying data of the impedance and of the phase shift between current and voltage (50 mV ac) in a frequency range of 1−10 MHz.

For the conductivity measurements the gases used were of highest purity and were supplied by Messer-Griesheim. Hydrogen was purified further by passing it through an oxygen-removing purifier, and helium was freed from traces of oxygen by an Anoxy-Cil unit. Condensable contaminants were removed from hydrogen and helium by liquid nitrogen traps, while oxygen was passed through a trap cooled with liquid nitrogen/ethanol.

3. Results

Oxygen-Treated Titania. The low-surface sample treated in a dry oxygen flow shows a rather simple dependence of the impedance on the frequency characterized by an ohmic resistance at low frequencies as is shown in the Bode plot (Figure 1). At high frequencies conduction is accomplished by a capacitance parallel to the resistance. With increasing temperature the low-frequency resistance of the titania decreases from about 300 MΩ at 623 K to about 25 MΩ at 723 K, the corresponding phase shift changes from 0° in the low-frequency region to −90° in the high-frequency region. The time constant of the overall process decreases from 16 ms at 623 K to 4 ms at 673 K and to 0.8 ms at 723 K. This short time constant indicates that this process may occur by electronic conduction.[24]

The corresponding Nyquist diagrams (Figure 2) shows a suppressed half circle and a small additional half circle at low frequencies. The suppression indicates that the process responsible for that circle is either characterized by a distributive element or is composed by two steps with a similar time constant. Simulation of the lefthand suppressed cycle using two serial RC contributions shows for all experiments perfect agreement with the experimental data. The time constant for the additional small half circle is typical for the electronic transfer between electrode and semiconductors.[25] Thus, a third RC element has to be added to describe the overall impedance.

The oxygen-treated high-surface sample shows a similar Bode plot at frequencies higher than 0.5 Hz (Figure 3a). Since our frequency range reached down to 0.01 Hz, we discovered an additional impedance contribution that increases with decreasing frequency. In this frequency range the phase shifts to negative values (Figure 3b) indicating that even at this low frequency an additional capacitor contributes to the total impedance. The time constant of the corresponding conduction process decreases with increasing temperature from 30 s at 698 K to 8 s at 723 K and to 0.4 s at 773 K, indicating an activated process. On the other hand, the height of the impedance step at this frequency increases with increasing temperature. This result contradicts the effect of temperature on the time constant, if the impedance contribution is considered to be in series with the electronic conduction steps discussed above. However, assuming the existence of a pathway parallel to the electronic conduction gives a consistent result. The time constant of the corresponding process is typical for diffusion phenomena and this conduction process is observed only with the high-surface sample. Thus, this pathway occurs most likely via ionic conduction along the surface of the titania particles. Because of this parallel pathway the Nyquist plot no longer gives direct information about the particular impedance elements. The separate contributions are obtained by fitting the data according to the circuit diagram derived from the given results.

The presence of water vapor also influences the impedance (Figure 4). When titania is treated in dry oxygen at room temperature the low-frequency impedance reaches the upper limit of resistance that can be measured with the used apparatus. Wet treatment, that is, with a water vapor pressure of 6.1 mbar in the oxygen gas, results in a decrease of the impedance by a

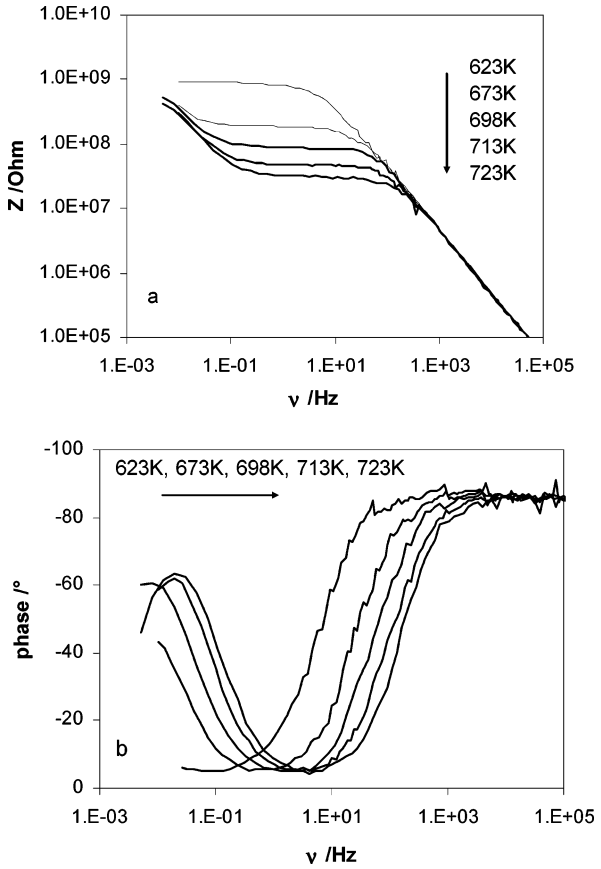

Figure 3. Bode diagrams of the oxygen-treated titania high-surface sample as a function of temperature: (a) modulus of impedance vs frequency, (b) phase shift vs frequency.

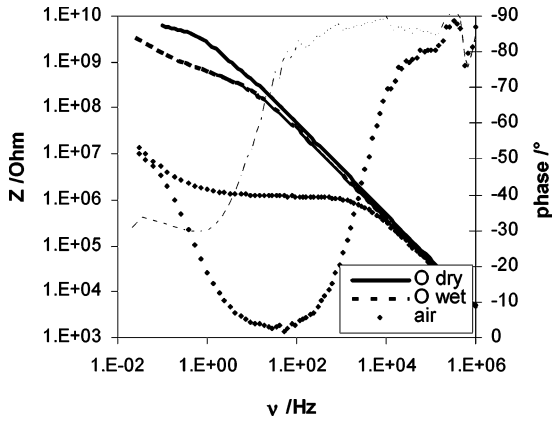

Figure 4. Effect of water vapor on the impedance (depicted as Bode diagrams) of the high-surface sample at room temperature.

factor of about five.[26] The time constant of the corresponding conduction process is similar to that of the additional pathway discussed above. This result supports the assumption that this pathway is due to ionic conduction. Most likely, bridged oxygen ions at the surface are converted to OH groups in the presence of water. As a consequence, the mobility of surface ions is increased due to charge transfer via hydrogen bridges.

Furthermore, when the sample is left in ambient air without any flow the impedance is smaller by three orders of magnitudes compared to treatment in dry oxygen. The effect of humidity on the impedance is stronger with the high-surface sample than with the low-surface sample. Under these conditions an additional conduction pathway may be opened since pore condensation of water may enable a charge transport in the liquid medium.

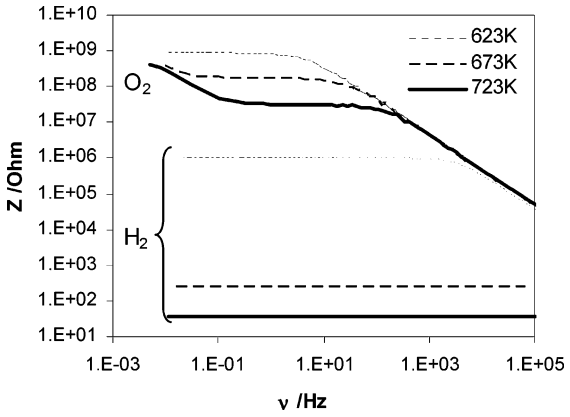

Figure 5. Bode diagrams of the high-surface sample treated either in oxygen or in hydrogen at 623 K, 673 K, and 723K (as indicated in the figure).

Hydrogen-Treated Titania. Far stronger changes in the impedance are obtained if titania is treated in flowing hydrogen instead of in oxygen. Figure 5 compares the impedance of the high-surface sample treated for 2 h in dry oxygen as well as in dry hydrogen at different temperatures. For the hydrogen-treated samples the impedance in the low-frequency region decreases from about 1 MΩ at 423 K to 200 Ω at 673 K and finally to about 30 Ω at 723 K. The time constant for the corresponding processes is the same as that for the electronic conduction in the oxygen-treated titania. This dramatic increase of the electronic conductivity is most likely caused by the formation of conduction electrons or electrons located in states slightly below the conduction band, which are formed in a superficial reduction of titania. In previous work[22] we were able to demonstrate that during hydrogen treatment below 723 K surface vacancies and electrons are formed via the equation

$$Ti^{4+}{}_s + O^{2-}{}_s + H_{2,g} \leftrightarrow Ti^{3+}{}_s + V_s + e^- + H_2O_g$$

or, if Ti^{3+} gives one electron to the donor sites in titania:

$$O^{2-}{}_s + H_{2,g} \leftrightarrow V_s + 2\,e^- + H_2O_g$$

The number of vacancies is controlled by a partial equilibrium between the surface and the gas phase, obeying the van't Hoff equation and resulting in a reaction enthalpy of 183 kJ/mol or 1.9 eV. From the dependence of the number of surface vacancies on the titania surface area it was concluded that the oxygen vacancies and the Ti^{3+} ions are remaining on the titania surface, while the electrons are distributed in the bulk. At a given temperature the number of electrons formed by reduction is controlled by the ratio of hydrogen partial pressure and the water vapor pressure. Thus, the withdrawal of water during treatment in dry hydrogen limits the further formation of charge carriers. A defined level of reduction can be obtained when titania is treated in hydrogen containing a controlled water partial pressure, as has been done in the wet treatments.

4. Discussion

Mechanism of Conduction. Considering all contributions to the overall impedance we propose the following scheme for the conduction mechanism occurring (i) via pathway A by electronic conduction and (ii) via pathway B by ionic transport (Figure 6).

The serial contributions of pathway A are each characterized by an ohmic resistor in parallel to a capacitor. In pathway B the ionic conduction along the titania surface is characterized

TABLE 1: Calculated Equivalent Data of the Oxygen-Treated Low-Surface Sample

	pathway A					pathway B		
T/K	R_b [kΩ.m]	C_b [pF]	R_{gb} [kΩ.m]	C_{gb} [pF]	R_{ct} [kΩ.m]	R_{sl} [kΩ.m]	W_{sl} [kΩ.m]	C_{sl} [nF]
623	276	33	742	91	132	1900	14 700	50
673	100	31	167	91	31	980	4300	50
698	68	31	71	104	15	550	5740	49
723	50	40	21	92	6.4	390	1300	51
873	0.8	40	0.33	92		97	250	50
1073	0.016	45	0.006	98	75×10^{-6}	28	40	50

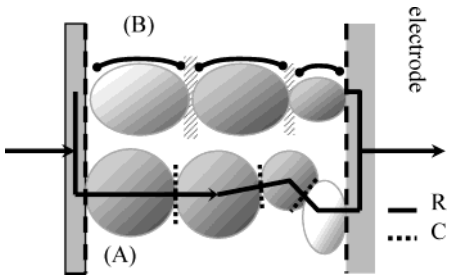

Figure 6. Scheme for the conduction mechanism.

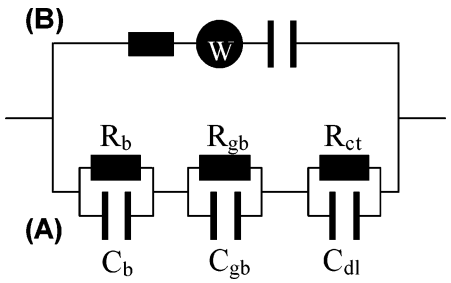

Figure 7. Circuit diagram equivalent to the conduction mechanism, subscripts of the RC combinations are b for bulk, gb for grain boundary, and ct for charge transfer at the electrode; R_i and W_i denote the ionic resistance and Warburg impedance, C_e, the ionic capacitance at the electrodes.

by a resistor. As the ions have to move along the grain boundaries over different distances, depending on the fractal structure of the grain surface, a simple resistor is not fully sufficient to simulate the surface conduction. Thus, for simulating the different diffusion paths along the grains we added a simple distributive impedance element, the Warburg impedance element, to the circuit diagram.

At the limit of low frequencies the impedance of pathway B increases and the phase shift changes to negative values (Figures 3a and 3b). The reason for this breakdown of the surface conduction may arise from ion blocking by grain boundaries perpendicular to the charge flow or by ion blocking at the interface to the gold electrode. In both cases this blocking is characterized by a capacitor in series to the resistor. The resulting equivalent circuit diagram is shown in Figure 7.

To prove the validity of the proposed mechanism we compared the experimentally obtained impedance spectra, depicted as Nyquist diagrams, with the impedance simulated from the circuit diagram (Figure 8). For some data the omission of any impedance element from the equivalent circuit may give sufficient agreement, but all elements of this circuit are necessary to describe all results obtained in this work. The agreement of the simulated spectra with the experimental data supports the validity of the circuit diagram. The simulation of the experimental data and their fitting to obtain optimum parameters allows us to calculate the individual impedance contributions.

Oxygen-Treated Samples. For the low-surface sample treated in dry oxygen the calculated values of the resistivity (related to the surface of the electrodes and the thickness of the pellet) and the capacitance of the several contributions are given in Table 1.

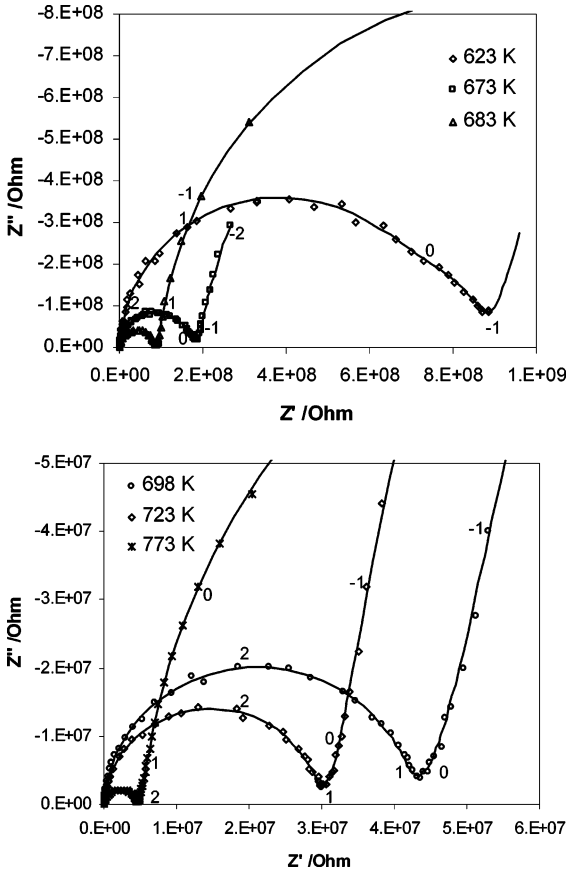

Figure 8. Nyquist spectra (data points) and simulated spectra (continuous line) of the high-surface sample treated in oxygen at 623 K, 673 K, 683 K (Figure 8a), 698 K, 723 K, and 773 K (Figure 8b).

In this sample the resistance of pathway B is higher than that of pathway A in the whole temperature range. The contribution of the ionic pathway to the dc conduction decreases from 6% at 623 K to 4% at 723 K and becomes negligible at 800 K. In pathway A the charge transport through the grain boundaries is the major contribution to the overall resistance below 700 K, while at higher temperatures the bulk conduction becomes rate limiting. The capacity parallel to the bulk resistivity remains constant below 700 K, the calculated value of the dielectric constant of 110 to 115 agrees well with the literature data of this sample consisting mainly of rutile (114 for powdered rutile[27]). Above 700 K the dielectric constant increases with increasing temperature, ending up in a value of 160 at 1073 K. Presumably, above 700 K the increasing number of charge carriers causes a more extensive charge shift in the alternating potential. On the other hand, the capacity parallel to the grain boundaries and the capacity in pathway B are nearly independent of the temperature, and the scatter of values expresses the error introduced by experiment and simulation.

TABLE 2: Calculated Equivalent Data of the Oxygen-Treated High-Surface Sample

	pathway A				pathway B		
T/K	R_b [kΩ.m]	C_b [pF]	R_{gb} [kΩ.m]	C_{gb} [pF]	R_{sl} [kΩ.m]	W_{sl} [kΩ.m]	C_{sl} [nF]
623	477	15	22 200	154	3000	132	51
673	220	14	4250	157	360	50	51
723	82	15	1000	155	98	22	50
773	44	16	230	152	21	11	51

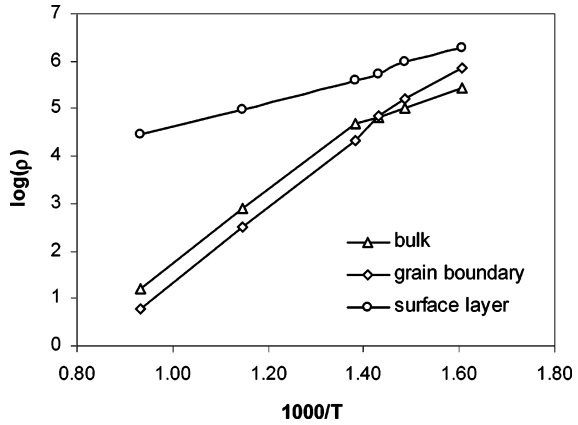

Figure 9. Resistive contributions to the impedance in the oxygen-treated low-surface sample as a function of temperature (Arrhenius diagram).

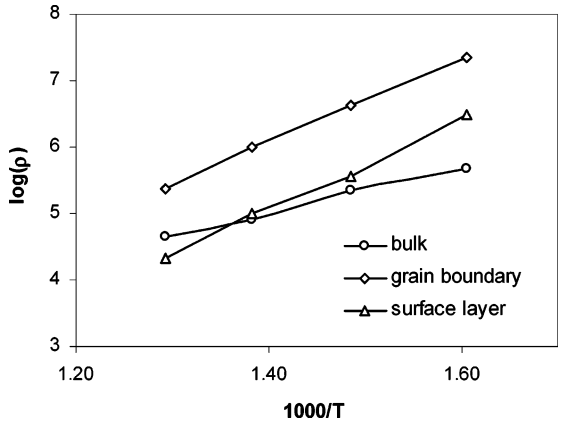

Figure 10. Resistive contributions to the impedance in the oxygen-treated high-surface sample as a function of temperature (Arrhenius diagram).

The Arrhenius diagram of the resistive contributions shows that the slope of the bulk resistivity changes at about 723 K (Figure 9). Thus, the mechanism of electronic conduction through the bulk may change at this temperature. Evaluation of this plot results in an apparent activation energy of 0.67 eV below 723 K and of 1.53 eV above 723 K.

This high-temperature activation energy is equal to the activation energy for the electronic transport through the grain boundaries, which is the rate-limiting conduction process in this temperature range.

The contribution of pathway B decreases with increasing temperature. The apparent activation energy for the ionic charge transport on the titania surface (0.54 eV) is much lower than that of the electronic conduction.

In the high-surface sample the proportion of pathway B becomes more important; about 90% of the conduction is due to this pathway (Table 2). The capacity corresponding to the blocking of the ionic transport is the same as in the low-surface sample. For the inhibition of charge transfer causing this capacitor two possibilities were proposed: (i) inhibition of ionic transfer between grains and (ii) inhibition of the ion discharge at the electrode. As the two samples exhibit the same capacitance independent of the particle size, we concluded that the ionic transport to the electrodes is blocked.

In pathway A of the high-surface sample the electronic conduction across the boundaries between grains or different phases becomes rate limiting because of the larger number of grain boundaries to be passed. The grain boundary capacity in the high-surface sample is higher than that in the low-surface sample by a factor of 1.7. Since the ratio of the mean crystallite diameter, revealed by X-ray diffraction line broadening, is 2.6, the grain boundary capacity should also be increased by this factor. The lower increase in capacity indicates that in the low-surface sample the mean distance between the grains is smaller because of pore collapse during the sintering process, resulting in a larger capacity contribution of each passed grain boundary.

The capacity parallel to the bulk resistance in the high-surface sample, which consists mainly of anatase, is much smaller than in the low surface sample. The corresponding value for the dielectric constant is about 55. This is in good agreement with the data given in the literature for anatase (50 for thin anatase films,[28] 55 for powders of TiO_2−P25,[29] and 48 for powdered anatase[30]). Up to the temperature limit of this sample the dielectric constant depends only slightly on the temperature.

Figure 10 shows the effect of temperature on the resistive contributions to the high-surface sample. In the now-prevailing pathway B the activation energy for ionic conduction is 1.35 eV; that is considerably higher than observed on the low-surface sample. Assuming that ionic transport across the grain boundaries is rate limiting in this pathway, the longer distance between the grains in the high-surface sample may cause a higher activation energy for ionic conduction. For electronic conduction in the bulk phase the apparent activation energy (0.67 eV) is the same as in the low-surface sample in the same temperature range. The barrier for electronic conduction across the grain boundaries is the same for both samples (1.25 eV), independent of the specific surface area.

Hydrogen-Treated Samples. After hydrogen treatment, the electronic conductivity of titania is extremely high and the pathway B no longer contributes to the overall charge transport. Consequently, the equivalent circuit given above only provides inaccurate parameters for pathway B. Furthermore, at higher temperatures the resistive elements of pathway A are so small that in the available range of ac frequency the parallel capacitive elements do not contribute to the overall impedance. Thus, the time constant of the three consecutive elements cannot be estimated and therefore a deconvolution of the impedance of pathway A into separate contributions gives only rough estimates, particularly in the high-temperature range. Tables 3 and 4 show the resistivity of the bulk and of the grain boundaries in the low-surface sample and in the high-surface sample, respectively, after treatment in hydrogen in the low-temperature range.

In the low-surface sample the bulk resistance is the limiting step for conduction, its dependence on the temperature results in an apparent activation energy of 0.73 eV. The activation

TABLE 3: Resistive Contributions of the Hydrogen Treated Low-surface Sample

treatment temperature T/K	bulk resistivity ρ/Ωm	grain boundary resistivity ρ/Ωm
373	75 000	16 300
423	5600	200
473	600	43
523	27	5

TABLE 4: Resistive Contributions of the Hydrogen-Treated High-Surface Sample

treatment temperature T/K	bulk resistivity ρ/Ωm	grain boundary resistivity ρ/Ωm
523	340	1 150 000
573	80	44 000
593	45	15 600
623	22	2300

energy for the charge transfer through the boundaries between the rutile grains is 0.95 eV.

In the high-surface sample the main contribution to the overall resistance comes from the charge transfer between the grains. The activation energy for this contribution (1.72 eV) is much larger than that for the low-surface sample. The enhanced activation energy may be due to the larger mean distance between the grains in the high-surface sample or due to the presence of two phases (anatase and rutile) in the high-surface sample.

The resistivity in the bulk phase obtained from the deconvolution seems to be higher in the high-surface sample by a factor of 10, at least at 523 K. The reason for this apparent contradiction may be that the high-surface sample consists partly of anatase, which exhibits a higher specific resistivity than rutile. However, in the high-surface sample this contribution is calculated from deconvolution beneath a 3000-fold higher grain boundary resistivity. Thus, the absolute value of bulk resistivity obtained by deconvolution may be erroneous. Nevertheless, the temperature effect on the bulk resistivity of this sample results in an apparent activation energy of 0.77 eV that agrees with the 0.73 eV found in the low-surface sample.

Energy Level of the Donor Sites. The apparent activation energy for bulk conduction (mean value 0.75 eV) is composed by the effect of temperature on the number of charge carriers and by the energy necessary to enable the hopping of electrons. This second contribution is mainly the energy gap between the donor sites and the conduction band. In the reaction given above, oxygen surface vacancies are formed together with electrons and/or with Ti^{3+} ions.

$$O^{2-}{}_s + H_{2,g} \leftrightarrow V_s + 2\,e^- + H_2O_g$$

Since in this reaction three lattice defects are formed, the energy needed for activation for one of this defects is one-third of the reaction enthalpy of 183 kJ/mol, that is, 61 kJ/mol or 0,63 eV.

The remainder of the apparent activation energy, about 0.12 eV, is thus the energy necessary to raise the electrons from their intergap sites to the conduction band.

At least above 723 K, the activation energy for bulk conduction in the oxygen-treated low-surface sample is 1.53 eV. In this high-temperature range the formation of oxygen vacancies should be possible even in an oxygen atmosphere. Assuming a vacancy formation similar to that in hydrogen, the following reaction should occur, as already proposed by Kevane:[2]

$$O^{2-}{}_s \leftrightarrow V_s + 2\,e^- + 1/2\,O_2$$

The enthalpy for this reaction is higher than that given above by the enthalpy of water formation, resulting a value of 430 kJ/mol or 4.45 eV. Thus, the energy contribution for formation of charge carriers in oxygen should again be one-third of this value, that is, 1,48 eV. The difference between the apparent activation energy for conduction and the energy of electron formation is 0.05 eV, that is the energy difference between the electonic intergap sites and the conduction band. Keeping in mind that the energy of the intergap sites was calculated from two different treatments at different temperatures, the two results (0.12 eV and 0.05 eV below the conduction band, respectively) agree within experimental error. This result corresponds to calculations of Chen et al.,[31] who proposed an electronic site due to a F^{2+} color center with an energy of 0.2 eV below the conduction band.

Below 723 K, the concentration of electrons in the oxygen-treated sample becomes rather low and conduction may occur by electrons arising from impurities in the bulk, connected with a far lower apparent activation energy, since their concentration is independent of temperature.

Conclusions

The electric charge transport in oxygen-treated titania (rutile) is most likely accomplished via two different routes. One pathway (A) occurs by electronic transport from the (gold) electrode to the titania grains, further through the bulk of these grains, and finally by electronic transport through grain boundaries perpendicular to the electric field. As a parallel pathway (B) surface ions can move along the grain surface parallel to the electric field and can surmount the grain boundaries between the grains. Because of the low voltage applied in the experiments, the ion discharge at the electrode is impeded, contributing a capacitive impedance only.

In the low-surface sample, treated in oxygen, the charge is transported mostly by electrons via pathway A. The electrons are formed by removal of surface oxygen ions, leaving a surface oxygen vacancy and two electrons in the titania. Since the formation of these charge carriers is highly endothermic, the apparent activation energy of this mechanism is higher than that of the ionic conduction and thus the ionic transport through the bulk becomes more important at lower temperatures. When the sample is treated under wet conditions, the rate of the ionic pathway becomes higher, most likely due to the presence of surface hydroxyl ions. In the oxygen-treated high-surface sample the ionic conduction prevails since more conduction channels can contribute to the ionic conduction because of the higher surface area.

When titania samples are treated in hydrogen the surface oxygen ions are removed more easily due to reaction with hydrogen. The apparent activation energy for electronic conduction becomes smaller because the enthalpy of vacancy formation is decreased by the formation energy of water. As a result, in hydrogen-treated titania the conduction is accomplished exclusively by electronic transport. By comparison of the enthalpy of vacancy formation and the apparent energy of bulk conduction, the true activation energy for electronic motion is calculated to be about 0.1 eV, that means that the electrons most likely occupy donor sites about 0.1 eV below the conduction band. Since the formation of these electrons depends on the fugacity

of oxygen, the impedance of titania can be used as a gas sensor for oxygen and hydrogen. Furthermore, the change of catalytic performance of titania supported noble metals by hydrogen treatment at elevated temperatures (SMSI-effect) may be due to the enhanced conductance of the support allowing a considerable charge transfer between the support and the metal.

References and Notes

(1) Herrmann, J.-M.; Pichat, P. *J. Catal.* **1982**, *78*, 425.

(2) Demmin, R. A.; Ko, C. S.; Gorte, R. J. *J. Phys. Chem.* **1985**, *89*, 1151.

(3) Knauth, P.; Tuller, H. L. *Solid State Ionics* **2000**, *136*−*137*, 1215−1224.

(4) Lazzeri, M.; Vittadini, A.; Selloni, A. *Phys. Rev. B* **2001**, *63*, 155409.

(5) Hollander, L. E.; Castro, P. L. *Phys. Rev.* **1960**, *119* (6), 1882−1885.

(6) Kevane, C. J. *Phys. Rev.* **1964**, *133* (5A), 1431−1436.

(7) Tuller, H. L. *Solid State Ionics* **2000**, *131*, 143−157.

(8) Poumellec, B.; Marucco, J. F. *J. Phys. Chem. Solids* **1986**, *47* (8), 831.

(9) Savage, N.; Chwieroth, B.; Ginwalla, A.; Patton, B. R.; Akbar, S. A.; Dutta, P. K. *Sens. Actuators, B* **2001**, *79*, 17−27.

(10) Göpel, W.; Reinhardt, G. Metal Oxide Sensors: New Devices Through Tailoring Interfaces on the Atomic Scale. In *Sensors Update Sensor Technology − Applications − Market*; Baltes, H., Göpel, W., Hesse, J., Eds.; VCH: Weinheim, 1996; p 49.

(11) Anderson, J. B. F.; Bracey, J. D.; Burch, R.; Flambard, A. R. 8th Inter. Congr. Catal., W−Berlin, 1984; 5, p 111.

(12) Bracey, J. D.; Burch, R. *J. Catal.* **1984**, *86*, 384.

(13) Vannice, M. A.; Twu, C. C. *J. Catal.* **1983**, *82*, 213.

(14) Herrmann, J.-M. Metal-titania catalysts. In *ACS Symposium Series: Strong Metal Support Interaction*; Baker, R. T. K., Tauster, S. J., Dumesic, J. A., Eds.; The American Chemical Society: Washington, 1986; p 200−211.

(15) Meriaudeau, P.; Ellestad, O. H.; Dufaux, M.; Naccache, C. *J. Catal.* **1982**, *75*, 243−250.

(16) Vannice, M. A.; Sudhakar, C. *J. Phys. Chem.* **1984**, *88*, 2429.

(17) Santos, J.; Phillips, J.; Dumesic, J. A. *J. Catal.* **1983**, *81*, 147.

(18) Tauster, S. J.; Fung, S. C.; Garten, R. L. *J. Am. Chem. Soc.* **1978**, *100*, 170.

(19) Burch, R. Strong metal support interactions. In *Hydrogen effects in catalysis*, Paal, Z., Menon, P. G., Eds.; 1988. p 347.

(20) Herrmann, J. M. *J. Catal.* **1984**, *89*, 404−412.

(21) Spichiger-Ulmann, M.; Monnier, A.; Koudelka, M.; Augustynki, J. Spectroscopic and electrochemical study of the state of Pt in Pt−titania catalysts. In *ACS Symposium Series: Strong Metal Support Interaction*; Baker, R. T. K., Tauster, S. J., Dumesic, J. A., Eds.; The American Chemical Society: Washington, 1986; p 212−227.

(22) Eder, D.; Kramer, R. *Phys. Chem. Chem. Phys.* **2003**, *5* (6), 1314−1319.

(23) Haerudin, H.; Bertel, S.; Kramer, R. *J. Chem. Soc., Faraday Trans.* **1998**, *94* (10), 1481−1487.

(24) *Impedance Spectroscopy: Emphasizing Solid Materials and Systems*; Macdonald, J. R., Ed.; John Wiley & Sons: 1987.

(25) Bauerle, J. E. *J. Phys. Chem. Solids* **1969**, *30*, 2657−2670.

(26) Bhowmik, S.; Constant, K. P.; Parker, J. C.; Ali, M. *Mater. Sci. Eng.* **1995**, *A204*, 258−266.

(27) Roberts, S. *Phys. Rev.* **1949**, *76* (8), 1215−1221.

(28) Goossens, A.; Zanden, B. v. d.; Schoonman, J. *Chem. Phys. Lett.* **2000**, *331*, 1−6.

(29) Krol, R. v. d.; Goossens, A.; Schoonman, J. *J. Electrochem. Soc.* **1997**, *144* (5), 1723−1727.

(30) Errera, J.; Ketelaar, H. *J. Phys. Radium* **1932**, *3*, 239.

(31) Chen, J.; Lin, L.-B.; Jing, F.-Q. *J. Phys. Chem. Solids* **2001**, *62*, 1257−1262.